Encyclopedia of Earthquake Engineering
DOI 10.1007/978-3-642-36197-5_403-1

Electrochemical Seismometers of Linear and Angular Motion

Vadim M. Agafonov[a]*, Alexander V. Neeshpapa[b] and Anna S. Shabalina[a]
[a]Center for Molecular Electronics, Moscow Institute of Physics and Technology, Moscow, Russia
[b]R-sensors LLC, Dolgoprudny, Russia

Synonyms

MET seismic sensors; Molecular electronic angular and linear seismometers; Molecular electronic transfer seismic sensors

Introduction

Traditionally seismic sensors use a mechanical system with moving solid-state inertial mass in combination with either velocity or displacement transducers. The latter convert mechanical motion of the inertial mass into the electrical signal. An alternative approach based on employment of liquid inertial mass and four-electrode electrochemical transducer with potential difference applied between the electrodes as a converter of the liquid motion into electrical signal was developed in recent years (Huang et al. 2013; Agafonov et al. 2014). Such devices are known as MET (molecular electronic transfer) or electrochemical sensors. Basically, the operation of the MET sensors uses the sensitivity of an interelectrode current in the electrochemical cell to the movement of a liquid electrolyte relative to the electrodes fixed on the sensor housing. Along with the solid-state electronics (charge transfer by electrons and holes in a solid conductor or semiconductor) and vacuum electronics (charge transfer by free electrons in an ionized gas or vacuum), the MET sensors could be considered as the third class of fundamental electronic devices, characterized by charge transfer via ions in solution – hence the older name of the sensing technology "Solion." Solion technology was first implemented into a practical device in the 1950s by a US Navy-sponsored project. The early applications of Solion devices were to detect low-frequency acoustic waves, either in the form of an infrasonic microphone or limited-band seismometer (Hurd and Lane 1957; Wittenborn 1958; Collins et al. 1964). The first theoretical model describing the physical principles of operation of such devices was developed by C. W. Larcam in 1965 (Larcam 1965) who studied a simple one-dimensional model of four electrodes (two anodes and two cathodes) placed along a channel filled with an electrolyte moving under the action of external inertial forces.

Significant work on Solion motion detectors was continued in Russia, where the term "molecular electronic transfer" was firstly introduced to describe such a device (Lidorenko et al. 1984). Inspired by the exceptionally high rate of mechanical signal conversion to electric current in MET involving mass and charge transport, pioneer studies of MET (Kozlov et al. 1991; Kozlov and Safonov 2003; Panferov and Kharlamov 2001; Reznikova et al. 2001; Agafonov and Krishtop 2004; Volgin et al. 2003) provided an alternative paradigm in the development of seismic sensors. The advantages of MET motion sensors include small size, lack of fragile moving parts, high shock tolerance, wide operating frequency range, high sensitivity, and low noise, as well as low dependence or complete independence of the response on installation angle. These features are widely used in practice especially in field and ocean-bottom

*Email: agvadim@yandex.ru
*Email: r-sensors@mail.ru

DOI 10.1007/978-3-642-36197-5_403-1

applications, giving important benefits in using a relatively non-expensive, easy to install, compact and at the same time sensitive and low-noise device.

The main part of the current paper includes the following divisions: operating principles, description of the method, how the transfer function is built, and examples of technical parameters for a commercial MET, including velocimeters, seismic accelerometers, and unique highly sensitive compact rotational seismometers.

Molecular Electronic Transducer: Principle of Operation

Figure 1 illustrates the basic concept of a MET sensing element, consisting of two transforming electrochemical cells (Lidorenko et al. 1984). Four electrodes configured as anode–cathode–-cathode–anode (ACCA), separated by dielectric spacers, which protect adjacent electrodes from contact, span the channels filled with an electrolyte containing iodide ions. Holes through the electrodes and dielectric spacers allow fluid to flow through the channels.

The sensing mechanism of the MET is based on reversible chemical reactions transferring charge between anode and cathode via the electrolyte ions in the solution (Sun and Agafonov 2010). A solution with a high concentration of a neutral electrolyte (taking no participation in the electrode reactions) and a small fraction of the active component that is responsible for the charge transport over the fluid–electrode metal interface is usually used.

Most of the practical devices use iodine–iodide electrochemical systems with platinum electrodes. The electrolyte consists of a high-concentration aqueous solution of potassium iodide *KI* (lower temperature range boundary at −15 °C) or lithium iodide *LiI* (lower temperature range boundary at −55 °C) as neutral electrolyte and a small quantity of molecular iodine I_2. If there is an excess supply of iodide, iodine enters a freely soluble complex compound (triiodide) according to the following scheme:

$$I_2 + I^- \rightarrow I_3^- \tag{1}$$

When the current flows through the MET, the following electrochemical reactions proceed at the electrodes: the reduction of iodine at the cathode

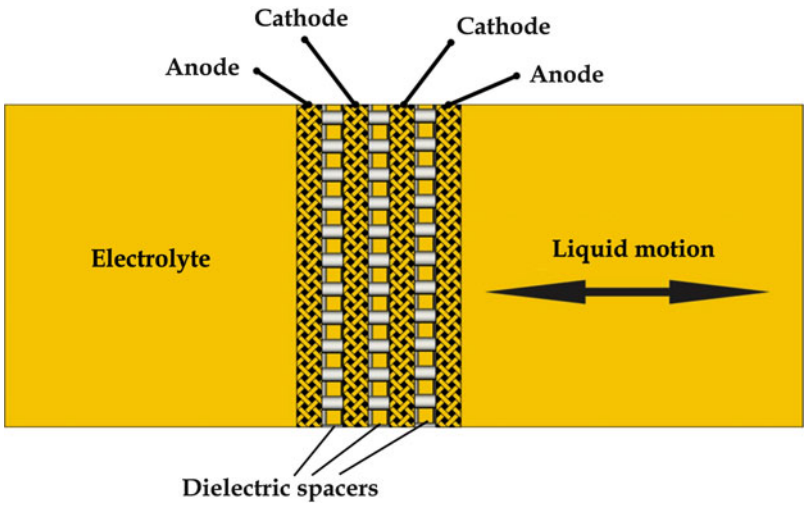

Fig. 1 Schematic of the basic MET sensing element

Encyclopedia of Earthquake Engineering
DOI 10.1007/978-3-642-36197-5_403-1

$$I_3^- + 2e^- \rightarrow 3I^- \tag{2}$$

and the oxidation of iodine at the anode

$$3I^- - 2e^- \rightarrow I_3^-. \tag{3}$$

K and *Li* ions do not participate in the reactions.

The sensing element operation is based on the fact that rates of the electrochemical reaction at the electrodes are significantly higher than the reactant supply rate. The electrode reactions in this case lead to the emergence of a reactant concentration gradient. Figure 2a shows the distribution of I_3^- and I^- in the stationary electrolyte. Because of the electrode reactions, triiodide concentration maximizes at the anodes and minimizes at the cathodes, while iodide concentration maximizes at the cathodes and minimizes at the anodes. Since the ion concentrations shown in Fig. 2a are symmetric about the central plane of the cell at $x = 250$ μm, left and right parts of the sensing element are equivalent, and there is no electric current difference between the two pairs of electrodes.

The ion distributions in the moving fluid are shown in Fig. 2b. From Fig. 2b, the maximum of the triiodide concentration is found at the upstream anode, while the minimum is at the downstream cathode.

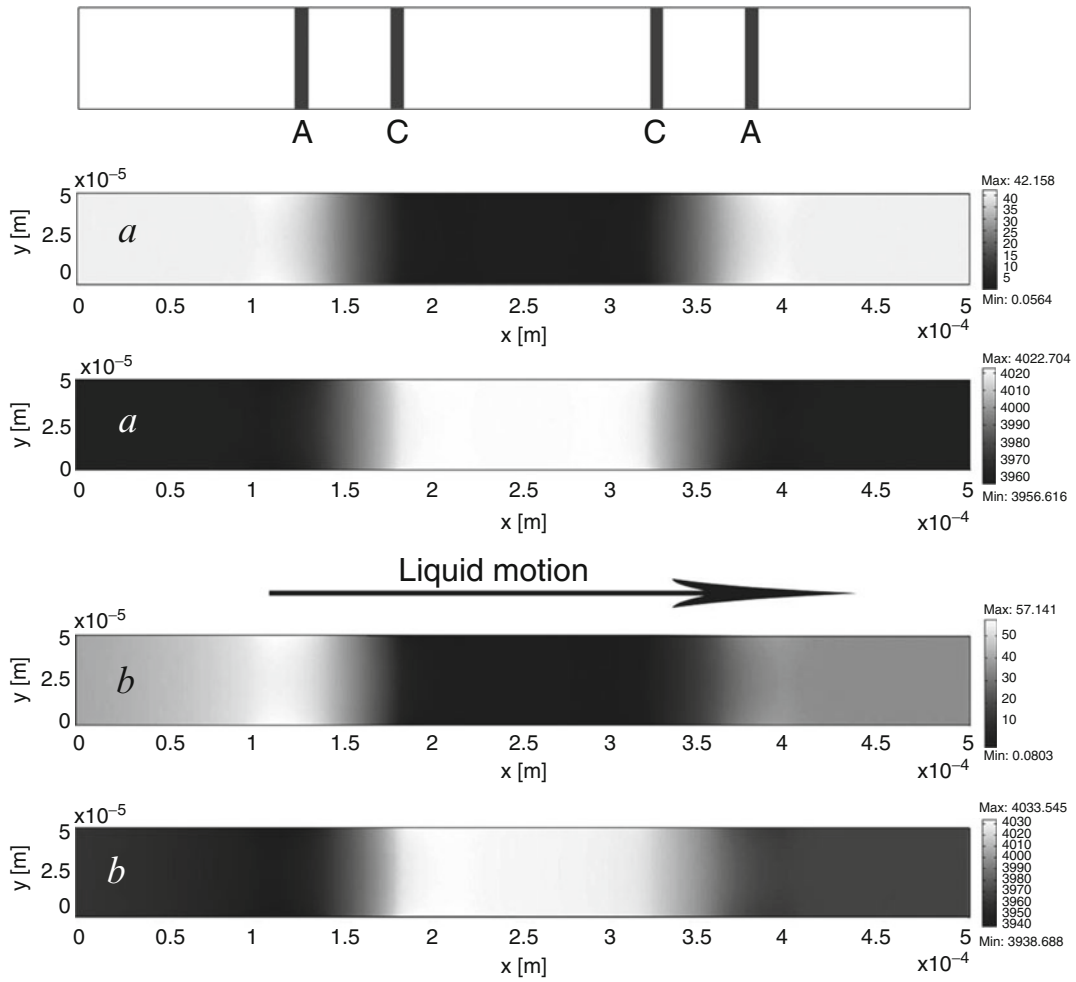

Fig. 2 Schematic diagram of a four-electrode conduit (the electrodes are denoted by the shaded portions) and ion distributions in (**a**) stationary and (**b**) moving electrolyte. Both in (**a**) and (**b**), I_3^- concentration is shown on the upper graph, I^- on the lower one

DOI 10.1007/978-3-642-36197-5_403-1

For iodide, as shown in Fig. 2b, the maximum concentration occurs at the upstream cathode, while the minimum concentration is found at the upstream anode. The maximums and minimums found in Fig. 2b are due to the fact that the triiodide generated at the upstream anode is consumed at the downstream cathode. By comparing Fig. 2a, b, it is found that both the maximum and the minimum concentrations of triiodide are greater when the fluid flows; for iodide the maximum concentration is greater when the fluid flows, while the minimum is greater in the stationary electrolyte. In turn, changes in the ion distribution result in the changes of the electrode current. Specifically, increase of the triiodide concentration in the vicinity of a cathode means acceleration of the electrochemical reaction according to Eq. 2. Inversely, decrease of the triiodide concentration results in the deceleration of the same reaction. So there is a difference between electrical currents for the two electrode pairs in the moving electrolyte. Usually the difference between cathode currents is used as an output signal of the transducer.

As the interelectrode potential difference is increased, the rate of electrochemical reactions increases gradually until such a condition occurs that all the triiodide ions reaching the electrode enter the electrochemical reaction instantly. This condition corresponds to the saturation current regime, and further increase in the potential difference does not alter the current. Under this condition the conversion coefficient of the sensing cell achieves its maximum value. That is why the saturation regime is typically used as a working point for the transducer. The current is limited by the volume rate of supply of the active component to the electrodes. In turn, the supply rate is determined by the ion diffusion in the stationary electrolyte. The flow of the solution introduces an additional convective ion transport that changes the saturation current at each pair of electrodes (see the volt–ampere characteristics (VACs) of the electrode system in the stationary and flowing electrolyte shown in Fig. 3). The convective flow is directed from cathode to anode for the first pair of electrodes and in opposite direction for the second one. That's why changes of the concentration are not symmetrical, and cathode current difference (output signal) is generated.

In the general case, the process is characterized by a high conversion factor. This is reflected in a strong electric response that exceeds the noise of accompanying electronic circuitry significantly, even when the input mechanical influence level is low. A high signal-to-noise ratio is ultimately achieved throughout the entire measurement channel. Numerous experimental and theoretical studies revealed a considerable dependence of the output parameters of the device on the conversion system geometry and the broad possibilities for optimizing the conversion system response depending on the problems being solved.

Motion sensors based on MET technology include linear and angular accelerometers, rate sensors, gyroscopes, and seismometers. MET sensors can be configured for horizontal, vertical, and rotational sensing, as shown in Fig. 4. Despite of the difference in construction, all of them can be described in common rules-based approach. A vertical-axis sensor is considered in the following as an example.

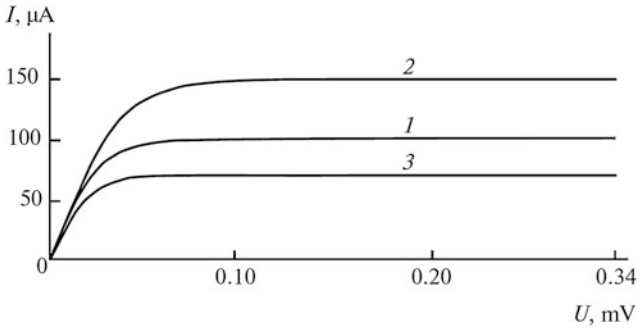

Fig. 3 VACs of the transducer electrode system in a stationary electrolyte (*1*) and in an electrolyte flowing from the anode to the cathode (*2*) and cathode to anode (*3*)

Encyclopedia of Earthquake Engineering
DOI 10.1007/978-3-642-36197-5_403-1

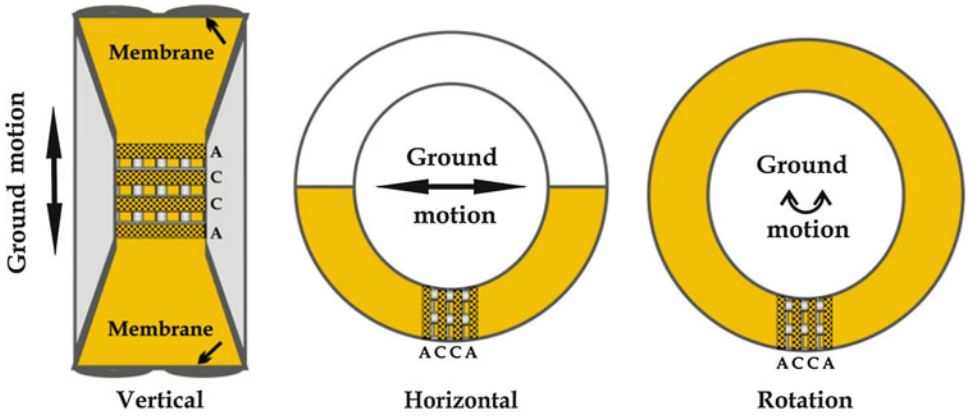

Fig. 4 Schematic of different type of MET motion sensor

Transfer Function of the MET Seismometers

A MET motion sensor can be considered as a superposition of two systems: first, input motion is converted into fluid motion of the electrolyte by a mechanical system. Next, the electrolyte's velocity is measured by the electrochemical system, resulting in an output current of the sensor. Therefore, the frequency-dependent transfer function of the entire device can be written as:

$$H(\omega) = H_{\text{mech}}(\omega) H_{\text{ec}}(\omega), \tag{4}$$

where $H_{\text{mech}}(\omega)$ describes the mechanical response of the fluidic system and $H_{\text{ec}}(\omega)$ is the electrochemical transfer function describing the conversion of the fluid flow into an output current.

Considering the design of the vertical sensor (Fig. 4a) in addition to the sensing element, the highly flexible rubber membranes are assembled at the two ends of the channel to seal the electrolyte, providing a restoring force for the mechanical system. In the presence of an external ground acceleration, an inertial driving force is applied on the liquid electrolyte. The electrolyte moves along the channel once the driving force exceeds the hydrodynamic drag force. Let $x(t)$ be the displacement of the liquid inertial mass m relative to the ground. There are two real forces acting on the liquid mass:

Restoring force from the flexible membrane, $-kV(t)$, is negative since it opposes the flow motion, where $V(t)$ is the volume of fluid passing through the channel and k is the flexibility coefficient of the membrane and depends only on the characteristics of the membrane.

Hydrodynamic damping force, $-\frac{R_{\text{h}} S_{\text{ch}} dV(t)}{dt}$, is linearly proportional to the volumetric flow rate of the liquid associated with the hydrodynamic resistance R_{h} and is negative since it also opposes the flow motion; S_{ch} is the cross-section area of the channel. In this consideration we suppose the cross-section area is constant.

The acceleration of the mass relative to an inertial reference frame will be the sum of the acceleration $\frac{d^2x(t)}{dt^2}$ with respect to the ground and the ground acceleration $a(t)$. The center of mass acceleration is assumed equal to average liquid acceleration in the channel. Since the sum of forces must be equal to the mass times the acceleration, the equation that governs the motion of the liquid can therefore be expressed as

$$-R_{\text{h}} S_{\text{ch}} \frac{dV(t)}{dt} - kV(t) = m \frac{d^2x(t)}{dt^2} + ma(t). \tag{5}$$

DOI 10.1007/978-3-642-36197-5_403-1

Given the relations:

$$V(t) = S_{\mathrm{ch}} x(t),\ m = \rho L S_{\mathrm{ch}}, \tag{6}$$

where m is the mass of the electrolyte, ρ is the density of the electrolyte, and L represents the channel length, Eq. 5 is transformed to

$$\frac{d^2V(t)}{dt^2} + \frac{R_{\mathrm{h}} S_{\mathrm{ch}}}{\rho L}\frac{dV(t)}{dt} + \frac{k}{\rho L}V(t) = -S_{\mathrm{ch}} a(t). \tag{7}$$

By changing the variable of $Q(t) = \frac{dV(t)}{dt}$, where $Q(t)$ is the volumetric flow rate, and transforming Eq. 7 to frequency domain, the magnitude of the transfer function of mechanical system in MET transducer in the frequency domain can be obtained as follows:

$$|H_{\mathrm{mech}}(\omega)| = \left|\frac{Q(\omega)}{a(\omega)}\right| = \frac{\rho L}{\sqrt{\left(\frac{\rho L}{S_{\mathrm{ch}}}\right)^2 \frac{(\omega^2 - {\omega_0}^2)}{\omega^2} + {R_{\mathrm{h}}}^2}}, \tag{8}$$

where $\omega_0 = \sqrt{\frac{k}{\rho L}}$ is the mechanical resonance frequency of the device.

An approximation of the electrochemical transfer function in frequency domain is

$$|H_{\mathrm{ec}}(\omega)| = \frac{1}{\sqrt{1 + \left(\frac{\omega}{\omega_D}\right)^2}}, \tag{9}$$

where $\omega_D = \frac{D}{d^2}$ is the diffusion frequency and d is the interelectrode distance (Kozlov et al. 1991).

The overall frequency-dependent transfer function of a MET seismometer is a superposition of the transfer functions of the mechanical and electrochemical system, which can be written as:

$$|H(\omega)| = \frac{\rho L}{\sqrt{\left(\frac{\rho L}{S_{\mathrm{ch}}}\right)^2 \frac{(\omega^2 - {\omega_0}^2)}{\omega^2} + {R_{\mathrm{h}}}^2}} \cdot \frac{1}{\sqrt{1 + \left(\frac{\omega}{\omega_D}\right)^2}}. \tag{10}$$

Figure 5 illustrates the typical response of a MET sensor to the applied acceleration (blue) and velocity (red). Both plots have marked maximums in sensitivity and do not have any flat region. To produce the flat response in the operating frequency range, a procedure of frequency equalization is required.

Two main approaches to equalize the frequency response of a MET sensor have been developed so far:

1. Equalization with a combination of low-pass and high-pass filters (filter equalization)
2. The use of force feedback (feedback equalization)

The filter equalization was used in earlier MET seismometers. The actual parameters of a specific sensing cell are difficult to predict and display a noticeable spread, so the task of achieving the desired accuracy can only be performed by means of the measuring the cell's transfer function directly. Shake tables of various types are necessary equipment to implement this procedure.

Encyclopedia of Earthquake Engineering
DOI 10.1007/978-3-642-36197-5_403-1

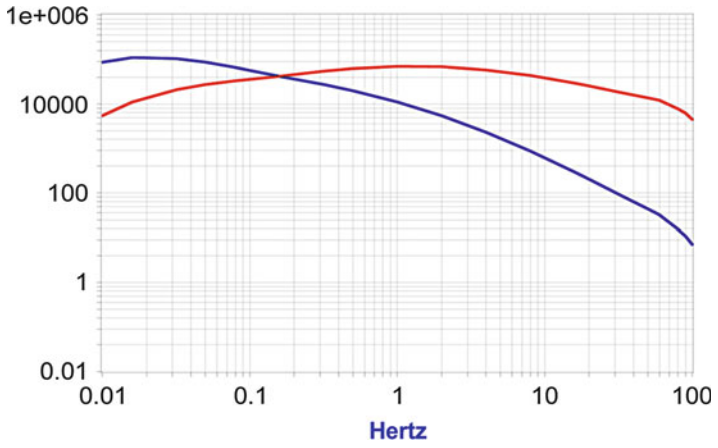

Fig. 5 Responses of a typical MET transducer to applied acceleration (*blue*) and velocity (*red*). Units on vertical axis are μA/m/s^2 and μA/m/s for the *blue* and *red curves*, correspondingly

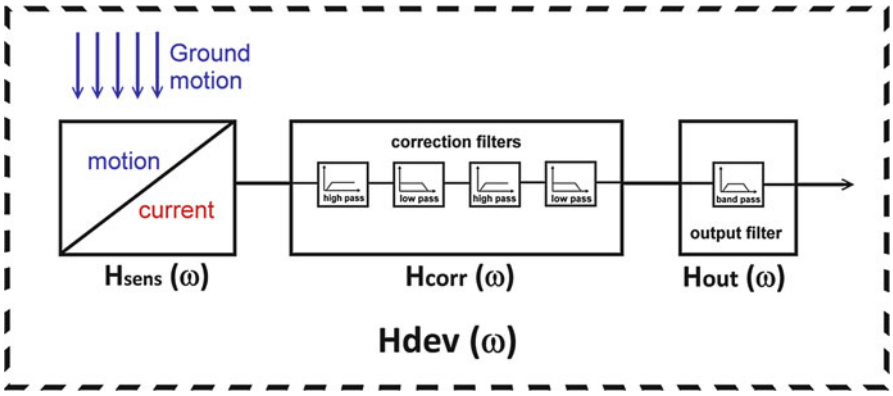

Fig. 6 Functional diagram of a seismometer with the filter equalization

The approach is based on the directly measured response of a particular sensing cell in the frequency range of interest and adjustment of the corrective filters to get the desired response in the specified operating frequency band.

Figure 6 presents the functional diagram for the seismometer where the transfer function was built using the filter equalization procedure. Mathematically, the transfer function of a seismometer $H_{\text{dev}}(\omega)$ is presented as a product of the transfer function of the transducer by the transfer functions of the successive electronic filters:

$$H_{\text{dev}}(\omega) = H_{\text{sens}}(\omega) \cdot H_{\text{corr}}(\omega) \cdot H_{\text{out}}(\omega). \tag{11}$$

The adjustment procedure is the following: First the seismometer transfer function is determined by measuring the seismometer response with some initial parameters of the correcting circuit. After that, the transducer transfer function is calculated by dividing the seismometer transfer function by a product of the electronic filter transfer functions:

$$H_{\text{sens}}(\omega) = \frac{H_{\text{dev}}(\omega)}{H_{\text{corr, initial}}(\omega) \cdot H_{\text{out}}(\omega)}. \tag{12}$$

DOI 10.1007/978-3-642-36197-5_403-1

After that the parameters of the correcting filters are remade using adjustable electronic parts. The mathematical modeling is used to find the required modifications. The result of the correction is checked on the shake table. If necessary, the adjustment procedure is repeated successively until the measured response function $H_{dev}(\omega)$ meets the standard curve within a tolerance predetermined as acceptable. The iterative adjustment process eliminates the influence of natural spread of electronic component values. The equalization procedure and the final result of the adjustment are illustrated on Fig. 7a–d, where real data are used as an example. The amplitude vs. frequency characteristics are shown, where Fig. 7a is the measured transfer function to applied velocity of the transducer, Fig. 7b is the transfer function for the electronic filters, Fig. 7c is the final amplitude vs. frequency curve, and Fig. 7d is the final phase vs. frequency curve for the seismometer.

The accuracy of the filter equalization procedure is limited by the tolerance of the electronic components and the accuracy of the shake table used to determine the transfer function. The usual variation in the transfer function for a broadband seismometer with filter equalization stays within ±1 dB for sensitivity and ±30° in the passband. What's more, the filter equalization is unable to correct any changes in the transducer's transfer function that may occur in the long term after the factory adjustment. Now this type of equalization is used only in a few models of electrochemical seismometers.

More precise devices use the feedback design. The commonly used technique for a practical feedback implementation is a moving coil system. The flexible membrane (see Fig. 4a) is equipped with a coil placed in a magnetic field of a firmly installed strong magnet. Applying a current into the coil gives rise to a force acting on the moving liquid inside the sensor. Usually, negative feedback is implemented, so that the force produced by the coil acts oppositely to the inertial force. It is important to note that for this approach, due to the high original conversion coefficient of the transducer, the decrease in the conversion factor due to the negative feedback, practically, does not affect the instrument resolution.

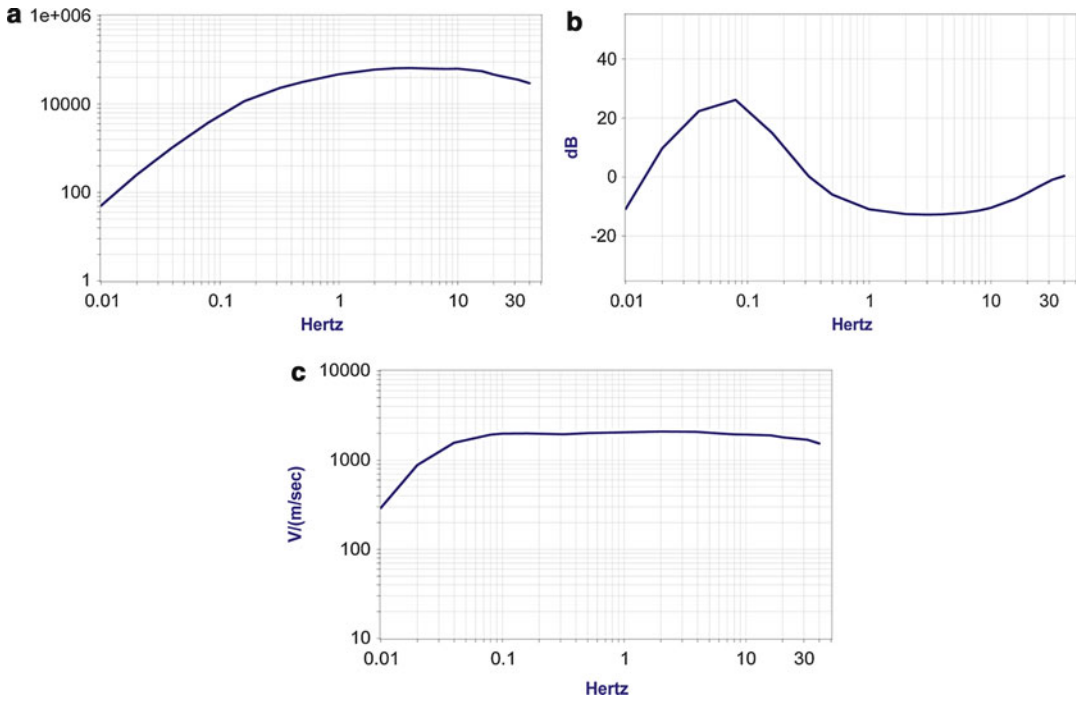

Fig. 7 (**a**) Transfer function $H_{sens}(\omega)$ of a horizontal MET transducer, (**b**) product of the transfer functions $H_{corr}(\omega) \bullet H_{out}(\omega)$ of equalization filters, (**c**) resulting transfer function $H_{dev}(\omega)$ of a horizontal MET seismometer

DOI 10.1007/978-3-642-36197-5_403-1

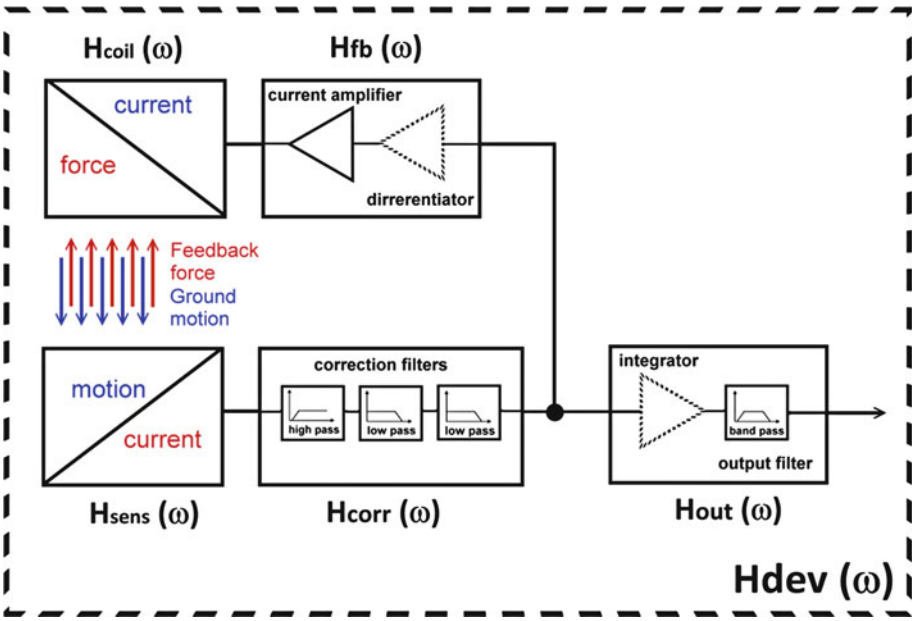

Fig. 8 Block diagram of a closed-loop electrochemical seismometer

The block diagram of the seismometer equipped with a feedback mechanism is presented in Fig. 8, where $H_{\text{corr}}(\omega)$ represents the transfer function of filters and amplifiers in direct circuit, $H_{\text{fb}}(\omega)$ is the same of the feedback circuit, and $H_{\text{out}}(\omega)$ is the transfer function of the output filter.

The most important feature of a feedback is that, provided the system remains stable and the amount of feedback is sufficient, the output function $H_{\text{dev}}(\omega)$ depends mostly on the feedback transfer function $H_{\text{fb}}(\omega) \cdot H_{\text{coil}}(\omega)$ rather than on the transducer transfer function $H_{\text{sens}}(\omega) \cdot H_{\text{corr}}(\omega)$.

Indeed

$$H_{\text{dev}}(\omega) = \frac{H_{\text{sens}}(\omega) \cdot H_{\text{corr}}(\omega)}{1 + H_{\text{sens}}(\omega) \cdot H_{\text{corr}}(\omega) \cdot H_{\text{fb}}(\omega) \cdot H_{\text{coil}}(\omega)} H_{\text{out}}(\omega). \tag{13}$$

In case the amplification inside the closed-loop system is much higher than 1 in absolute value $|H_{\text{sens}}(\omega) \cdot H_{\text{corr}}(\omega) \cdot H_{\text{fb}}(\omega) \cdot H_{\text{coil}}(\omega)| >> 1$ and Eq. 13 is approximated by the following formula:

$$H_{\text{dev}}(\omega) = \frac{1}{H_{\text{fb}}(\omega) \cdot H_{\text{coil}}(\omega)} H_{\text{out}}(\omega). \tag{14}$$

The feedback circuit results in a counterforce (i.e., a force compensating effect of the acting acceleration) proportional to the current flow. So $H_{\text{coil}}(\omega)$ can be expressed as a function that converts voltage to acceleration.

The practical implementation of the electrochemical seismometer equipped with feedback is:

Task 1: Providing sufficient amplification to have a "deep" feedback

Actually, this is the simplest task among others listed below. First, the transducer itself has a high original conversion factor. Additionally, the electronic industry produces a variety of low-noise operational amplifiers which can be used for additional amplification of a signal.

Task 2: Producing an output proportional to either acceleration or velocity, depending on the instrument type

DOI 10.1007/978-3-642-36197-5_403-1

In case the electronics in the feedback has frequency-independent response, the transfer function of the instrument would be proportional to acceleration. The output filter transfer function $H_{\text{out}}(\omega)$ is used to shape the low- and high-cutoff frequencies.

A velocimeter is more common for broadband seismometers. In this case, an additional circuit, an integrator as a part of the output filter ($H_{\text{out}}(\omega) \sim \frac{1}{\omega}$ in the passband), or a differentiator at the feedback amplifier ($H_{\text{fb}}(\omega) \sim \omega$ in the passband) should be added (both shown in dashed lines in Fig. 8).

Whenever an integrator or differentiator is used, the transfer function of the instrument would give an output voltage proportional to the ground velocity.

The introduction of an integrator into circuits at lower frequencies is limited by electronic parts leakage and op-amps offset. Also, the substantial variation of capacitors' impedance over the passband in frequency-dependent circuits may impair the noise performance of a device. Therefore special schematic techniques and careful amplifier selection should be made in order to maintain the optimal noise performance of the integrator or differentiator stage.

Another aspect of introducing a differentiator into the feedback circuit is that it brings a leading $\pi/2$ phase shift in the loop amplification. Typically, this phase shift improves feedback stability, and velocimeters with a differentiator in the feedback have better performance at higher frequencies in comparison with devices equipped with an output integrator.

Task 3: Ensuring the stability of the closed-loop system

Maintaining the feedback loop stable is a comparatively sophisticated task. Being negative in the middle of the frequency band, the feedback may even change its sign and become positive at some frequency outside the high- or low-frequency band limits due to the phase response variation as a function of frequency. To avoid self-oscillation, it is important to keep the amplification inside the closed-loop system at such a frequency less than 1 in absolute value by all means. This task not only requires considerations of stability when the system is being adjusted, but it's also essential to maintain the closed-loop stable over all temperature ranges and under transitions processes after the device is just powered on or overloaded by a strong input signal.

Changes of an electrochemical seismometer frequency response with variation of the feedback depth are illustrated in Fig. 9. The device response at a low feedback depth is close to the curve of an uncorrected sensor with no visible flat region at all. The deeper the feedback, the wider is the flat region in the device response, but at the same time the lower is the overall sensitivity of the device. Very strong

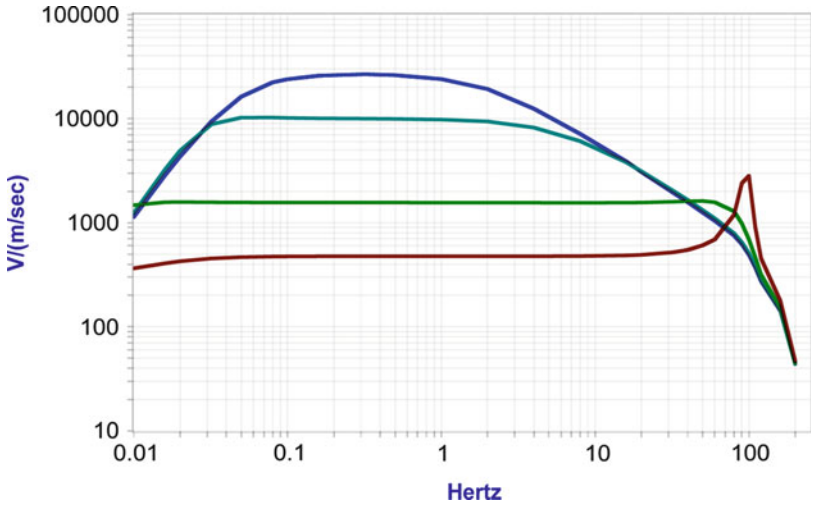

Fig. 9 Device response vs. feedback depth (depths 1, 5, 40, 120)

DOI 10.1007/978-3-642-36197-5_403-1

feedback depth (dark red curve on the Fig. 9) could result in the feedback loop becoming unstable during the transition processes or under variations in temperature.

Most electrochemical seismometers have maximum feedback depth in the range from 10 to 50. The feedback for the electrochemical accelerometers could be as big as few hundred.

Task 4: Sufficiency in feedback dynamic range

For the sake of keeping the dynamic range at a maximum, the feedback amplifier should provide sufficient current into the coil. The main limitation comes from the fact that modern systems are continuously using a lower and lower voltage supply, while coil size and weight of the moving body cannot be correspondingly reduced. Moreover, a heavier moving body of a sensor gives less thermal self-noise. A low-noise seismometer usually needs a larger current for the feedback coil.

The procedure of adjusting a sensor with feedback equalization consists of two stages. During the first step, a proper frequency response is made paying no attention to actual device sensitivity. In the second step, the required device sensitivity is adjusted.

The open-loop characteristics can be obtained by means of an external digital-to-analog converter (DAC) and analog-to-digital converter (ADC) with a harmonic response scan. The frequency response of the open loop outside the operational range is essential to ensure the system stability. After the initial open-loop response is obtained, the filter correction is made to adjust the feedback amplification, to make a flat response in the passband and predetermined behavior at low- and high-cutoff frequencies. The process is iterative in the same way as it was for the non-feedback devices.

The main difference compared to the non-feedback case is that the adjusting procedure gives a much more accurate response of a seismometer within the passband than for the non-feedback sensor. Generally the high- and low-cutoff frequencies are extended by 2–3 octaves. In parallel with the feedback adjustment, a fine-tuning of the output filter is done. In case the closed-loop response is actually flat over the passband, the device characteristics coincide with the output filter characteristics. This decreases the complexity of further device response presentation in terms of poles and zeroes.

The last step in manufacturing the device is the adjustment of its sensitivity. The operation can be carried out by adjusting the overall gain of the output filter's $H_{\text{out}}(\omega)$.

After this final adjustment, the resulting frequency response characteristic of a closed-loop device is measured and verified. The main point of this method is in simulating ground motion by adding of an external signal into the closed-loop circuit. This signal addition works in the same way as a real input signal. An external sine wave generator can be used to provide such a signal at various frequencies and thereby get a full calibration function.

The block diagram of the closed-loop calibration procedure is illustrated in Fig. 10 where the sine wave test signal from a generator is added to the closed-loop signal in the summation unit $\sum$. The signal disturbance introduced into the closed-loop and the output response are measured by an external 2 channel analog-to-digital converter.

The examples of the resulting calibration curves are shown in Figs. 11 and 12.

The closed-loop calibration procedure makes the subsequent maintenance and validation of a device possible with a common DAC–ADC and a reference sensor with verified sensitivity and noise performance. The test is carried out only by means of the standard device connector and does not require any intervention into the sensor or disassembling the device. The presence of a shake table becomes unnecessary. The device sensitivity can be determined using either factory-determined calibration constants or by analyzing the simultaneous recording made with a sensor with known sensitivity. The noise performance of a device can only be obtained by analyzing the simultaneous record made by at least two sensors placed close to each other. One of the approaches is to calculate non-correlating components in the signal of two sensors of the same type with identical parameters (sensitivity, phase response, passband). Another approach is to make simultaneous recording with a

DOI 10.1007/978-3-642-36197-5_403-1

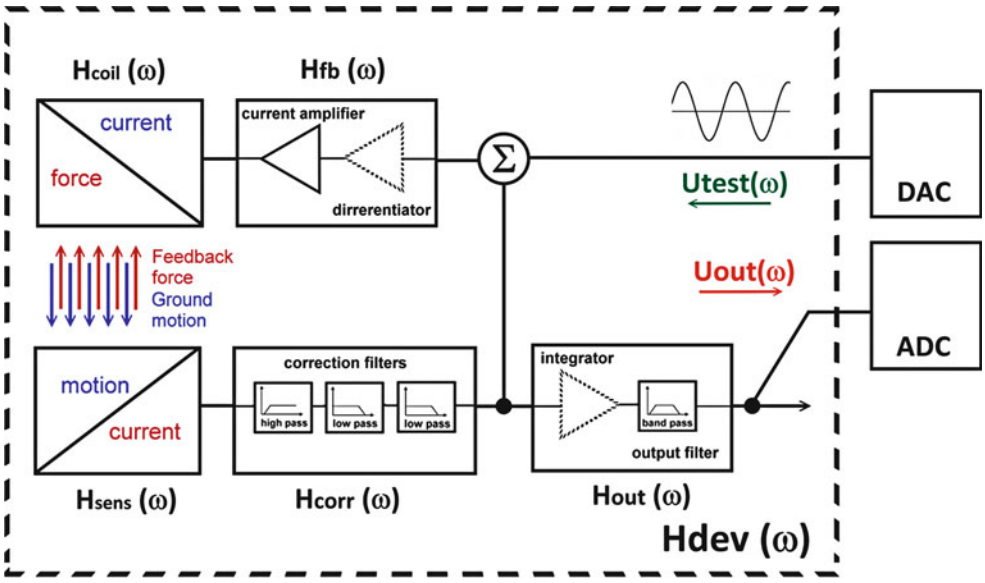

Fig. 10 Closed-loop self-calibration

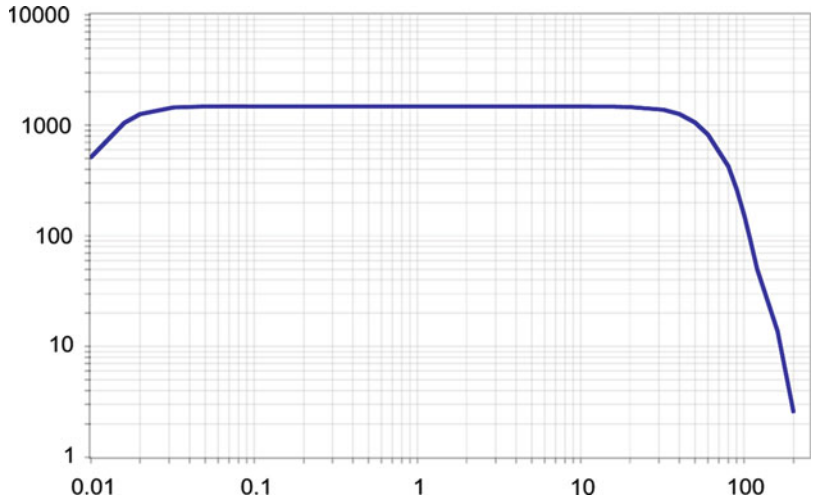

Fig. 11 Seismometer response obtained by the self-calibration test. The actual CME-6011 sensor was used to generate an example

sensor with far better noise performance. In the latter case the noise can be calculated by subtracting the low-noise sensor's signal from the tested sensor's signal.

Overview of Commercial Electrochemical Seismometers

Broadband Seismometers

The MET seismometers available cover a wide area of applications from permanent seismic stations to seismic field surveys, borehole measurements, and autonomous ocean-bottom systems (OBS). All devices are characterized by robustness, reliability, light weight, and easy installation procedure. None of them require any type of mass lock in transportation or mass centering during installation. They are

DOI 10.1007/978-3-642-36197-5_403-1

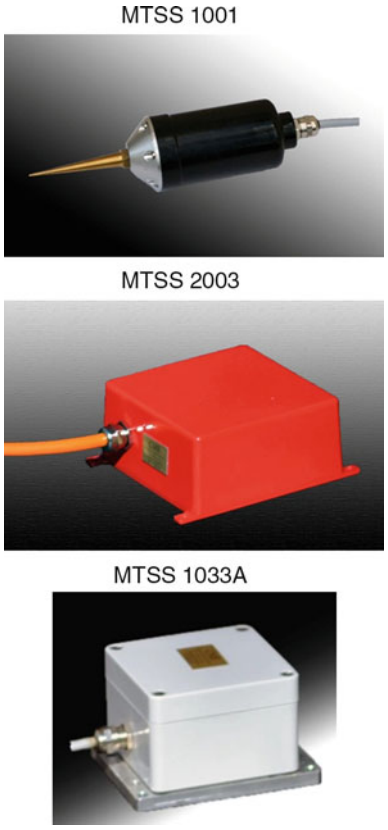

Fig. 12 MET geophones and accelerometers

operable under tilts up to ±10° and more, and some models are able to operate under any tilt angles. This feature is extremely useful for OBS operation. The lightest and the most power-efficient models of three component seismometers like CME-4211OBS have weight of 2.2 kg and power consumption of 90 mW during operation. The dynamic range for the best models is in the range 135–150 dB, while self-noise of the devices goes down below the lowest observed vertical seismic noise levels estimated by the New Low Noise Model (NLNM) in the 15 s–1 Hz range. The majority of models are equipped with closed-loop force feedback equalization. However, devices with filter equalization are lighter and use less power, which is essential for self-contained systems.

Seismometers for permanent installation have better noise performance due to heavier moving parts and are therefore more complex in design. These devices have the lowest cutoff frequency and due to that are less suitable for portable applications. However, for vault installation such parameters as power consumption and weight have less significance. Like other MET devices, they don't require any special arrangements during installation and operation. Models designed for self-contained systems, like field geological surveys with frequent location changes or for oceanic exploration, feature energy effectiveness, light weight, and compact size. Low-frequency cutoff as high as 0.1 Hz is more common for these instruments (Tables 1 and 2).

MET-Based High-Sensitive Geophones and Seismic Accelerometers

The main advantages of MET-based seismic geophones and accelerometers with negative feedback lie in their extremely high coefficient of conversion of mechanical motion into an electrical signal, the possibility of a significant (compared to a traditional geophone) expansion of the frequency range both in the low- and high-frequency directions, and the simplicity and reliability of the design (Agafonov

Table 1 The comparison chart for MET sensors for permanent seismic stations (sensors are sorted in alphabetical order)

Sensor type, producer, country	BB603 PMD Scientific, Inc., USA http://www.pmdsci.com/pdfs/BB603.pdf	CME-6211, R-sensors LLC, Russia http://www.r-sensors.ru/1_products/Descriptions/CME-6211.pdf	EP-300, Eentec, USA http://www.eentec.com/EP-300_data.htm
Operating principle	Electrochemical transducer	Electrochemical transducer	Electrochemical transducer
Equalization type	Force-balancing feedback	Force-balancing feedback	Force-balancing feedback
Output signals	Triaxial	Triaxial	Triaxial
Sensitivity	2,000 V/(m/s)	2,000 V/(m/s)	2,000 V/m/s
Frequency bandwidth	Standard: 0.0167–50 Hz	Standard: 0.0167–40 Hz	Standard: 0.0167–50 Hz
	Optional: 0.0083–50 Hz	Optional: 0.0083–40 Hz	Optional: 0.0083–50 Hz
Maximum output swing	±10 V	±20 V	±10 V
	(±20 V_{p-p} differential)	(±40 V_{p-p} differential)	(±20 V_{p-p} differential)
Self-noise	Below USGS NLNM in 0.05–5Hz range	Below NLNM in 0.1–7 Hz band	Below NLNM in 0.9–12 Hz band
Temperature range	Standard −12 °C to +55 °C	Standard −12 °C to +55 °C	Standard −12 °C to +55 °C
		Extended −40 °C to +55 °C	
Nominal supply voltage, consumption	Standard: 12Vdc, 28 mA	Standard: 12Vdc, 55 mA	Standard: 12Vdc, 30 mA
	Low power: 12Vdc, 12 mA	Low power: 12Vdc, 27 mA	Low power: 12Vdc, 12 mA
Mass lock, centering	None required	None required	None required
Maximum installation tilt	±10°	±15°	±10°
Case diameter/height	200 mm/220 mm	272 mm/240 mm	200 mm/220 mm
Weight	11 kg	12 kg	11 kg

Table 2 The comparison chart for seismic MET sensors for field work (sensors are sorted in alphabetical order)

	BB313	CME-4211	CME-6011	MP403
Sensor type, manufacturer	PMD Scientific, USA http://www.pmdsci.com/pdfs/BB313.pdf	R-sensors, Russia http://www.r-sensors.ru/1_products/Leaflets/4211.pdf	R-sensors, Russia http://www.r-sensors.ru/1_products/Descriptions/CME-6011.pdf	PMD Scientific, USA http://www.pmdsci.com/pdfs/MP403.pdf
Operating principle	Electrochemical motion transducer	Electrochemical motion transducer	Electrochemical motion transducer	Electrochemical motion transducer
Equalization type	Force-balancing feedback	Vertical: force-balancing feedback Horizontal: filter equalization	Force-balancing feedback	Force-balancing feedback
Output signals	Triaxial	Triaxial	Triaxial	Triaxial
Sensitivity	Standard: 2,000 V/(m/s)	Standard: 2,000 V/(m/s)	Standard: 2,000 V/(m/s)	Standard: 2,000 V/(m/s)
Frequency bandwidth	Standard: 0.033–50 Hz	Standard: 0.033–50 Hz Optional: 0.1–100 Hz	Standard: 0.033–40 Hz Optional: 0.1–50 Hz	Standard: 0.1–50 Hz
Maximum output swing	±10 V (±20 Vp–p diff.)	±15 V (±30 Vp–p diff.)	±20 V (±40 Vp–p diff.)	±10 V (±20 Vp–p diff.)
Temperature range	Standard −12 °C to +55 °C	Standard −12 °C to +55 °C	Standard −12 °C to +55 °C	Standard −12 °C to +55 °C
		Extended −40 °C to +55 °C	Extended −40 °C to +55 °C	
Nominal supply voltage, consumption	Standard: 12Vdc, 28 mA	Standard: 12Vdc, 27 mA	Standard: 12Vdc, 26 mA	Standard: 12Vdc, 28 mA
	Low power: 12Vdc, 12 mA	Low power: 12Vdc, 8 mA	Low power: 12Vdc, 10 mA	Low power: 12Vdc, 12 mA
Mass lock, centering	None required	None required	None required	None required
Maximum installation tilt	±12°	±15°	±15°	±12°
Case diameter/height	155 mm/185 mm	180 mm/140 mm	204 mm/210 mm	200 mm/220 mm
Weight	5.5 kg	4.3 kg	6.6 kg	9 kg

DOI 10.1007/978-3-642-36197-5_403-1

et al. 2010; Agafonov et al. 2014). Until recently, the instruments of this kind were used almost exclusively for measurements in the low-frequency domain. However, the developments of recent years (Krishtop et al. 2012) have made it possible to produce the devices with an upper operating frequency that exceeds the values typical for most geophones.

The experience learned from the development of such sensors indicates that the optimal operating characteristics are attained when MET-based sensors are equipped with an electrodynamic negative feedback mechanism. With a feedback, the instrument scale factor of 300 V/m/s is achieved without using any additional amplification, which is equal to or greater than that achieved by other known low-frequency geophones. At the same time, for a frequency range starting at 1 Hz, the MET geophones are much smaller than typical electrodynamic geophones.

The external view of sensors is shown in Fig. 12. MTSS-1001 is a single-axis, ultracompact, high-gain, 1-Hz seismic sensor. MTSS-2003 contains three orthogonal oriented MTSS-1001 seismic sensors. It is probably the world's smallest tri-axis 1-Hz seismometer. MTSS-2003 is designed primarily for measuring small low-frequency signals. It combines high gain, small size, and low power consumption.

The 3-component high-performance accelerometer MTSS-1033A and its 1-component version MTSS-1031A are designed for strong motion seismic measurements, industrial vibration monitoring, vibration isolation analysis, etc. MET accelerometers combine very small size and high sensitivity over wide frequency band. The wide dynamic range, low distortion, high temperature stability, and competitive price make it ideal and cost-effective solution for various applications such as earthquake, strong motion measurements, or structural monitoring. At the same time, unlike mechanical force-balanced accelerometers, the MET accelerometers cannot measure the DC component of the seismic signal. Although, the seismic signal is oscillating, the DC signal has a significant practical importance. The DC signal makes it possible to calibrate the sensor by rotating or tilting it relative to the gravity vector and to determine the sensor's axes orientation with respect to the vertical direction. In addition, the difference in low-frequency phase behavior makes it difficult to compare the responses of a MET accelerometer and a mechanical DC accelerometer (Table 3).

Electrochemical Angular Motion Seismometers

Interest in the pure rotational seismometer is driven by the suggestion that adding a new type of measurements would allow to better characterize the response of the structures to seismic input, to measure more accurately the seismic field spatial distribution, to be able separate between modes of

Table 3 The technical performance parameters for MET compact low-frequency geophones and accelerometers

Performance	MTSS-1001	MTSS-1041A	MTSS-1031A
Frequency range	1–300 Hz	0.1–120 Hz	0.1–120 Hz
Sensor noise	150 nm/s, rms over frequency range	110 ng/√Hz	150 ng/√Hz
Conversion factor	250 V/(m/s)	6 V/g	2.4 V/g
Maximum negative feedback depth	20	100	150
Maximum applied acceleration	–	±2 g	±4 g
Dynamic range	>110 dB	>110 dB	>120 dB
Non-linearity	<1 %	<1 %	<1 %
Orientation	Any direction	Any direction	Any direction
Weight	180 g	180 g	180 g
Temperature	"−55 ~ +65 °C"	"−55 ~ +65 °C"	"−55 ~ +65 °C"
Power	<80 mW	<80 mW	<80 mW

DOI 10.1007/978-3-642-36197-5_403-1

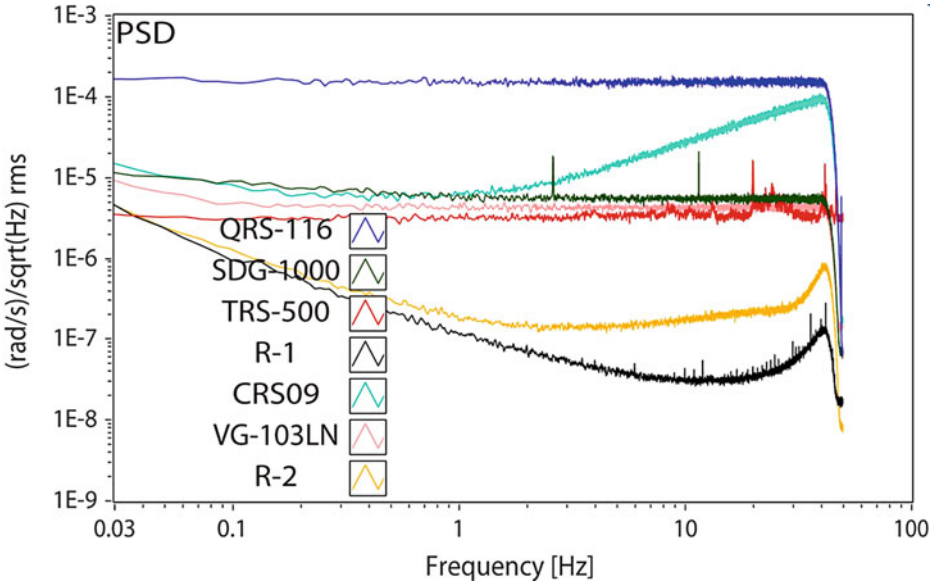

Fig. 13 Comparison of the self-noise for some electrochemical angular seismometers (models R1 and R2) with other angular motion sensors (Lin et al. 2013). The models QRS-116, SDG-1000, and CRS-09 are angular motion sensors based on MEMS technology. The TRS-500 and VG-103LN are fiber-optic gyros

Table 4 Technical parameters of commercially available rotational seismometers

Model	METR-03/01, LLC R-sensors, http://www.r-sensors.ru/1_products/Seismic_sensors_METR-03_CME-106C.pdf, R1 eentec, http://www.eentec.com/R-1_data_new.htm;	R2, Eentec, (Bernauer et al. 1012)	METR-13/11, LLC R-sensors, http://www.r-sensors.ru/1_products/Seismic_sensors_METR-03_CME-106C.pdf,
Output	Angular rate	Angular rate	Angular rate
Sensor type	Electrochemical	Electrochemical	Electrochemical
Noise at 1 Hz	10^{-7} rad/s/√Hz (for R1, see Fig. 13)	$2*10^{-7}$ rad/s/√Hz (see Fig. 13)	
Full-scale range	0.1 rad/s	0.3 rad/s	0.1 rad/s
Bandwidth	0.033–50 Hz	0.033–50 Hz	1–150 Hz
Size	120 × 120 × 102	120 × 120 × 102	120 × 120 × 102

seismic waves based on their polarization, and to determine better the site effect (Lee et al. 2011; Bernauer 2012a; Kapustian et al. 2013). Detailed information can be found at web page www.rotational-seismology.org, especially devoted to different aspects of the seismic rotational measurements for a variety of applications. A special issue "Advances in rotational seismology: instrumentation, theory, observations, and engineering" was issued in Journal of seismology, volume 16, # 4 in October 2012.

The mechanical configuration of the rotational seismometer, based on the electrochemical sensing technology, is presented in Fig. 4 above. The sensor consists of the toroidal channel, filled with an electrolyte, and the sensitive cell placed across the channel, converting liquid motion into the electrical response. An expansion volume is used to compensate for the temperature expansions of the liquid.

DOI 10.1007/978-3-642-36197-5_403-1

Electrochemical sensors are probably the only rotational sensors which are commercially available at a reasonable cost with a resolution appropriate to seismic applications. Figure 13 shows the spectral noise density spectrum of rotational electrochemical sensors compared with other commercial devices measuring rotation. The parameters of some of the commercially available electrochemical rotational seismometers are shown in Table 4. The independent test data can also be found in Bernauer et al. (2012b).

Summary

The electrochemical seismometers offer an alternative to regular electromechanical devices. They are compact, robust, and easy to install and provide good quality data. The operation principles of the electrochemical seismometers are based on using the charge transfer variations due to electrolyte motion in the four-electrode electrochemical cell. Among the commercial devices developed on the base of this technology are broadband seismometers, compact high-sensitive MET geophones, accelerometers, and unique angular seismometers.

Cross-References

- ▶ Broadband Seismometers
- ▶ Downhole Seismometers
- ▶ Ocean Bottom Seismometer
- ▶ Seismic Accelerometers
- ▶ Sensors, Calibration of Essay

References

Agafonov VM, Krishtop VG (2004) Diffusion sensor of mechanical signals: frequency response at high frequencies. Russ J Electrochem 40:537–541

Agafonov VM, Egorov EV, Zaitsev DL (2010) Molecular electronic linear accelerometers. Preliminary test results. Gyroscopy Navigation 1(4):246–251

Agafonov VM, Egorov IV, Shabalina AS (2014) Operating principles and technical characteristics of a small-sized molecular–electronic seismic sensor with negative feedback. Seismic Instrum 50(1):1–8

Bernauer M, Fichtner A, Igel H (2012a) Measurements of translation, rotation and strain: new approaches to seismic processing and inversion. J Seismol 16(4):669–681

Bernauer F, Wassermann J, Igel H (2012b) Rotational sensors—a comparison of different sensor types. J Seismol 16:595–602. doi:10.1007/s10950-012-9286-7

Collins JL, Richie WC, English GE (1964) Solion infrasonic microphone. J Acoust Soc Am 36:1283–1287

Huang H, Agafonov V, Yu H (2013) Molecular electric transducers as motion sensors: a review. Sensors 13:4581–4597. doi:10.3390/s130404581

Hurd RM, Lane RN (1957) Principles of very low power electrochemical control devices. J Electrochem Soc 104:727–730

Kapustian N, Antonovskaya G, Agafonov V, Neumoin K, Safonov M (2013) Seismic monitoring of linear and rotational oscillations of the multistory buildings in Moscow. Geotechnical Geological Earthquake Eng 24:353–363

DOI 10.1007/978-3-642-36197-5_403-1

Kozlov VA, Safonov MV (2003) Self-noise of molecular electronic transducers. Tech Phys 48:1579–1582

Kozlov VA, Korshak AN, Petkin NV (1991) Theory of diffusion-type transducers for ultralow electrolyte flow-rates. Sov Electrochem 27:16–21

Krishtop VG, Agafonov VM, Bugaev AS (2012) Technological principles of motion parameter transducers based on mass and charge transport in electrochemical microsystems. Russ J Electrochem 48(7):746–755

Larcam CW (1965) Theoretical analysis of the solion polarized cathode acoustic linear transducer. J Acoust Soc Am 37:664–678

Lee WHK, Evans JR, Huang B-S, Hutt CR, Lin C-J, Liu C-C, Nigbor RL (2011) Measuring rotational ground motions in seismological practice. Information sheet. IS 5.3. Feb 2011; doi:10.2312/GFZ.NMSOP-2_IS_5.3

Lidorenko NS, Ilin BI, Zaidenman IA, Sobol VV, Shchigorev IG (1984) An introduction to molecular electronics. Enegoatomizdat, Moscow

Lin C-J, Liu G (2013) Calibration and applications of a rotational sensor www.iris.edu/hq/sits_13_docs/mon/Lin.pptx

Panferov AP, Kharlamov AV (2001) Theoretical and experimental study of an electrochemical converter of a pulsing electrolyte flow. Russ J Electrochem 37:394–398

Reznikova LA, Morgunova EE, Bograchev DA, Grigin AP, Davydov AD (2001) Limiting current in iodine–iodide system on vertical electrode under conditions of natural convection. Russ J Electrochem 37:382–387

Sun Zh, Agafonov VM (2010) 3D numerical simulation of the pressure-driven flow in a four-electrode rectangular micro-electrochemical accelerometer. Sensors Actuators B Chem 146:231–238. www.elsevier.com/locate/snb

Volgin VM, Volgina OV, Bograchev DA, Davydov AD (2003) Simulation of ion transfer under conditions of natural convection by the finite difference method. J Electroanal Chem 546:15–22

Wittenborn AF (1958) Analysis of a logarithmic solion pressure detector. J Acoust Soc Am 30:683–683